Archives of Biochemistry and Biophysics
Vol. 369, No. 1, September 1, pp. 181–192, 1999
Article ID abbi.1999.1347, available online at http://www.idealibrary.com on IDEAL®

Purification, Properties, and Amino Acid Sequence of a Hemoglobinuria-Inducing Phospholipase A_2, MiPLA-1, from *Micropechis ikaheka* Venom

Rong Gao,* R. Manjunatha Kini,† and P. Gopalakrishnakone*,†,[1]

**Venom & Toxin Research Group, Department of Anatomy, Faculty of Medicine, and † Bioscience Centre, Faculty of Science, National University of Singapore, 10 Kent Ridge Crescent, Singapore 119260, Singapore*

Received April 28, 1999, and in revised form June 16, 1999

Dark-colored urine is one of the clinical symptoms of envenomation by *Micropechis ikaheka* (New Guinea small-eyed snake). We have purified a phospholipase A_2, MiPLA-1, which induces dark-colored urine in experimental mice, to homogeneity. The analysis of the dark-colored urine by electrophoresis and N-terminal sequence determination indicated that the color of mouse urine is due to hemoglobin in the urine but not myoglobin. MiPLA-1 is the first hemoglobinuria-inducing toxin. Insignificant hemolytic activity of MiPLA-1 indicates that hemoglobinuria is not due to lysis of erythrocytes by MiPLA-1. This suggests that hemoglobinuria induced by MiPLA-1 may be due to kidney leakage caused by unknown mechanisms. MiPLA-1 also showed other biological effects, including myotoxicity as well as anticoagulant and antiplatelet effects. Structural studies show that MiPLA-1 is a basic protein with a molecular mass of 14041.60 ± 1.78 as determined by electrospray mass spectrometry. We have determined the complete amino acid sequence of MiPLA-1. It is a 124-amino-acid protein with a "pancreatic loop" and belongs to group IB phospholipase A_2 enzymes. Two short segments flanked by proline brackets are found in the sequence of MiPLA-1. These segments are on the surface of the molecule and hence may be involved in protein–protein recognition.

Key Words: **snake venom; phospholipase A_2; hemoglobinuria; amino acid sequence.**

The New Guinea small-eyed snake (*Micropechis ikaheka*) is a dangerous elapid. It is widely distributed in monsoon forests, rainforests, swamps, and coconut palm plantations throughout New Guinea and adjacent islands. It is a much more dangerous reptile than currently believed. Only its secretive nocturnal nature prevents more human envenomation. There have been many human fatalities due to their bites (1, 2). The clinical features of envenomation include peripheral neurotoxicity, anticoagulation, generalized muscle pain/tenderness, and dark urine (1). These symptoms suggest the presence of several toxic factors in the venom that interfere with neuromuscular transmission, blood coagulation, and muscle damage. Earlier, we isolated several long-chain and short-chain neurotoxins from this venom (3). These toxins may be the main reason for peripheral neurotoxicity. The venom is also rich in phospholipase A_2 (E.C. 3.1.1.4, PLA_2[2]) activity, and the PLA_2 isoenzymes are possibly responsible for anticoagulant and myotoxic effects (4, 5). However, the toxins inducing dark urine have not yet been identified. It is also not clear whether the dark color of the urine is due to myoglobin or hemoglobin.

Snake venom PLA_2s, in addition to their probable role in digestion of the prey, show a wide variety of pharmacological effects, including neurotoxicity (6), myotoxicity (7), and cardiotoxicity (8) as well as anticoagulant (9), antiplatelet (10), convulsant (11), hypotensive (12), hemolytic (13), hemorrhagic (14), and edema-inducing (14, 15) effects. Some of the venom PLA_2s are also known to induce dark urine. Takasaki *et al.* reported that several PLA_2 enzymes purified from

[1] To whom correspondence should be addressed. Venom & Toxin Research Group, Department of Anatomy, Faculty of Medicine, National University of Singapore, 10 Kent Ridge Crescent, Singapore 119260, Singapore. Fax: (65) 7787643. E-mail: antgopal@nus.edu.sg.

[2] Abbreviations used: PLA_2, phospholipase A_2; PVDF, polyvinylidine difluoride; TFA, trifluoroacetic acid; PRP, platelet-rich plasma; PE, S-pyridylethylated; LM, light microscopy; CK, creatine phosphokinase.

0003-9861/99 $30.00

Pseudechis australis venom induced hemoglobinuria in mice (16). However, there was no experimental evidence to show the presence of hemoglobin in the urine. In contrast, Mulgotoxin and *P. australis* VIII A, PLA_2 toxins isolated from *P. australis* venom, induce dark urine and the dark color of the urine is due to severe myotoxicity and myoglobinuria (17, 18). Therefore, it is possible that the other PLA_2 enzymes from *P. australis* also induce myoglobinuria but not hemoglobinuria. It has been shown that the myoglobinuria-inducing toxin purified from *P. australis* venom causes indirect nephrotoxic effects through myoglobin casts in kidney tubular system (19, 20). So far, no PLA_2 or toxin is shown to induce hemoglobinuria.

In our preliminary studies, *M. ikaheka* venom was fractionated by gel filtration on a Superdex 30 column and the fractions with PLA_2 activity were found to induce muscle damage, antiplatelet and anticoagulant effects, as well as dark-colored urine. In this paper, we report the isolation and purification of a hemoglobinuria-inducing PLA_2 enzyme from this venom. We have determined its complete amino acid sequence and its biological effects.

MATERIALS AND METHODS

Materials

The lyophilized *M. ikaheka* venom was obtained from the Venom Supplies, Australia. The prepacked UNO S1 column, precast gradient gel (10–20%), lower range molecular weight markers, and the polyvinylidine difluoride (PVDF) membrane were from Bio-Rad Laboratories (U.S.A.). The prepacked Superdex 30 column (Hiload 16/60) and the Sephasil C8 and C18 columns were from Pharmacia (Sweden). Collagen for platelet aggregation was from Chrono-log (U.S.A.). Male Swiss albino mice (18–22 g) and New Zealand Albino rabbits (2.5–3.5 kg) were from Animal Holding Centre, National University of Singapore. Mouse hemoglobin, dog myoglobin, and horse myoglobin were from Sigma (U.S.A.). Acetonitrile was purchased from Fisher Scientific (UK), while 4-vinlypyridine and trifluoroacetic acid (TFA) were purchased from Fluka Chemika-Biochemika (Switzerland). All other reagents were of analytical grade.

Assay for Phospholipase A_2 Activity

The phospholipase A_2 activity was determined by titration with 20 mM NaOH on a 718 STAT Titrino pH-stat (Switzerland) at room temperature and pH 8.0 following the method of Kawauchi *et al.* (21). An aqueous emulsion of 20 mM phosphatidylcholine in the presence of different concentration of $CaCl_2$ was used as substrate.

Molecular Mass Determination by Electrospray Mass Spectrometry

Sample was dissolved in 50% acetontrile and analyzed using Perkin–Elmer Sciex API 300 triple quadrupole instrument equipped with an ionspray interface. The ionspray voltage was set to 4600 V. The orifice voltage was set at 30 V. Nitrogen gas was used as the curtain gas with a flow rate of 0.6 liters/min, while compressed air was used as a nebulizer gas. The masses of protein and peptide samples were determined by flow injection analysis at a flow rate of 50 μl/min using Shimadzu 10 AD pumps as the solvent delivery system.

Capillary Electrophoresis

Capillary electrophoresis was performed on a BioFocus 3000 capillary electrophoresis system (Bio-Rad). The sample was injected to a 25-μm $\times$ 24-cm coated capillary using the pressure mode (5 psi/s) and run in 0.1 M phosphate buffer (pH 2.5) under 12.00 kV from + to − at 15°C for 10 min. Migration was monitored at 200 nm.

Urine Analysis

Different doses of toxin (dissolved in 100 μl of 50 mM Tris–HCl, pH 7.4 buffer) were injected into the experimental mice in the tail vein to examine the toxic effects. Tris–HCl buffer (50 mM Tris–HCl, pH 7.4) was used as control. To analyze the urine, the experimental mice were anesthetized and the urine samples were obtained directly from the bladder 2 h after injection. SDS–PAGE analysis of mouse urine was performed in a Bio-Rad precast gradient gel (10–20%). Samples were pretreated in 2.5% SDS and 5% β-mercaptoethanol at 100°C for 10 min. After electrophoresis, the protein bands were transferred to PVDF membrane and stained with Coomassie blue. The N-terminal sequence of specific protein was determined as described below.

Assay of Hemolytic Activity

Hemolytic activity was assayed on citrated mouse blood (collected in 3.8% sodium citrate, 1:9, v/v) or washed erythrocytes (washed three times with 20 mM Tris–HCl, pH7.4, containing 1 mM $CaCl_2$ and 0.9% NaCl and resuspended with 10 times the same buffer). The erythrocytes were incubated with different concentrations of toxin at 37°C for 30 min. The degree of hemolysis was determined as the percentage of hemoglobin released (measured at 540 nm) by the toxin compared with a 100% hemolysis by the addition of 1% Triton X-100.

Myotoxic Activity and Light Microscopy (LM)

Mice were anesthetized with ether, and a single im injection of various amounts of the toxin in 100 μl of 0.9% (w/v) sodium chloride was given into the calf muscle. Control mice received 100 μl of 0.9% (w/v) sodium chloride. Blood samples were collected from the right ventricle 3 h after injection. The blood samples were incubated for 2 h at 37°C and centrifuged to obtain the serum. The creatine phosphokinase (CK) activity of serum was determined using Sigma Kit K520. CK activity was expressed in Units/ml, where 1 Unit is defined as the amount of enzyme that phosphorylates 1 nmol of creatine per minute at 25°C. To examine the morphological alterations, the calf muscle was removed, postfixed overnight in 10% formalin, dehydrated through a series of ethanol, and finally embedded in wax. Sections of 7 μm thickness were cut and stained with hematoxylin and eosin (H&E) and examined under light microscope (Leitz Aristoplan). Areas exhibiting pathological changes were photographed with Kodak film.

Assay of Anticoagulant Effects

The anticoagulant effects of purified protein were characterized by three different clotting time measurements as described below.

Prothrombin time assay. To assay the prothrombin time, 100 μl citrated rabbit plasma and 100 μl 50 mM Tris–HCl, 0.1 M NaCl, pH 7.4 (containing different concentrations of toxin) were incubated at 37°C for 3 min. Clotting was initiated by the addition of 200 μl thromboplastin with calcium (Sigma), and clotting time was recorded using a BBL fibrometer from Becton Dickinson (U.S.A.).

Stypven time assay. Stypven time measurements were determined according to the method of Williams and Esnouf (22) with modification. Citrated plasma (100 μl) was incubated with 10 μl purified Russell's viper venom Factor-X-activating enzyme (0.04 U/ml, Sigma) and various amounts of toxin (in 100 μl of 50 mM Tris–HCl, 0.1 M NaCl, pH 7.4) for 3 min. After incubation, clotting was initiated by addition of 50 μl of 50 mM $CaCl_2$.

Thrombin time assay. Citrated plasma (100 μl) and 100 μl of 50 mM Tris–HCl, 0.1 M NaCl, pH 7.4 (containing different concentrations of toxin), were incubated at 37°C for 3 min. Clotting was initiated by the addition of 50 μl of standard thrombin reagent (0.01 NIH units).

Platelet Aggregation

Platelet-rich plasma (PRP) was prepared as the supernatant from citrated rabbit blood (in 0.38% sodium citrate) by centrifugation at 120*g* for 10 min at 22°C. A platelet suspension (in Tyrode's buffer) was prepared by following the method of Marrakchi *et al.* (23). Platelet aggregation was measured at 37°C by light transmission according to Born (24), using a Chrono-Log Model 500-CA aggregometer. PRP or washed platelets (250 μl) incubated with toxin or an equal volume of sample buffer was stirred at 1000 rpm, 37°C, for 3 min prior to the addition of the aggregation inducer. The reaction was monitored for 5 min, and the extent of aggregation was expressed as the percentage of control (in the absence of the toxin).

Reduction and Pyridylethylation of Protein

Protein (100 μg) was dissolved in 400 μl of denature buffer (6.0 M guanidinium hydrochloride, 0.13 M Tris, 1 mM EDTA, pH 8.0) containing 0.07 M β-mercaptoethanol. The mixture was incubated at 37°C for 2 h. Then a 1.5-fold molar excess (over sulfhydryl groups) of 4-vinylpyridine was added and incubated at 37°C. After 2 h, the PE-protein was desalted on the C8 column.

Digestion and Separation of Degenerated Peptides

Digestion of PE-protein with endoproteinase Lys-C and Glu-C was performed in 100 mM Tris–HCl, pH 8.5 (containing 4 M urea), in a molar ratio of 50:1 (PE-protein:proteinase) at 37°C for 24 h. Cyanogen bromide treatment was performed following the method described by Diaz *et al.* (25). The digests were purified on a Sephasil C18 column on a Smart System (Pharmacia) using a linear gradient of acetonitrile in 0.1% TFA.

N-Terminal Amino Acid Sequence

The N-terminal amino acid sequence of PE-protein and its peptides was determined by automatic Edman degradation using an Applied Biosystem 494 pulsed liquid-phased sequencer.

RESULTS

Isolation and Purification of MiPLA-1

Dark urine is one of the clinical features observed in snake-bite victims (1). In our preliminary studies, *M. ikaheka* venom was found to be highly toxic to experimental mice. All experimental mice died within 1 h after i.v. injection (1.0 μg/g body wt or higher). At these doses of crude venom, no significant dark urine was observed in experimental mice. This difference could be due to species specificity. To identify the toxins that induce the dark urine, the crude venom was fractionated on a Superdex 30 column. As shown in Fig. 1A, six peaks were obtained. Both PLA_2 activity and the dark-urine-inducing effect were found in peak 2, while neurotoxic activity was mainly found in peak 3 and 4. Then peak 2 from Superdex 30 was applied on an UNO S1 column equilibrated with 50 mM Tris–HCl, pH 7.4, buffer and the elution was achieved with a linear NaCl gradient. Ten protein peaks were obtained (Fig. 1B). The proteins in peaks 1, 4, and 9 possessed higher PLA_2 activity than other peaks and induced dark urine in experimental mice with similar potency. LC-MS examination of these three peaks indicated that several PLA_2 isoenzymes with similar molecular mass and hydrophobicity were found in peaks 1 and 4, while peak 9 was composed of one main component with a trace contamination (data not shown). Therefore, we selected peak 9 for further purification. One PLA_2 enzyme was purified by applying peak 9 of the UNO S1 column to a Sephasil C8 HPLC column and designated as MiPLA-1 (Fig. 1C). After three steps, 1.5 mg of MiPLA-1 was purified from 100 mg of crude venom.

Both capillary electrophoresis and mass spectrometry indicated that MiPLA-1 was homogeneous (Fig. 2). All subsequent experiments on biochemical and biological characterization were performed using only purified MiPLA-1. The molecular mass of MiPLA-1, determined by mass spectrometry analysis, was 14041.60 $\pm$ 1.78 with a $pI > 10.4$ as determined by capillary isoelectric focusing.

Phospholipase A_2 Activity

The phospholipase A_2 activity of MiPLA-1 was examined under different concentrations of Ca^{2+}. In Ca^{2+}-free solution, MiPLA-1 did not show any significant PLA_2 activity. With the addition of Ca^{2+}, the hydrolytic activity increased rapidly (see Fig. 3). MiPLA-1 binds to Ca^{2+} with an apparent K_d of 0.12 mM. This affinity to Ca^{2+} is similar to the values previously described for 14-kDa secretory PLA_2s (26, 27). The specific activity of MiPLA-1 was estimated to be 283 μmol/min/mg (under 10 mM $CaCl_2$). In comparison with the PLA_2 isoenzymes (specific activities ranging from 75 to 10,000 μmol/min/mg) purified from the venom of *P. ausralis* (16), MiPLA-1 was a weak PLA_2 enzyme.

Hemoglobinuria Induced by MiPLA-1

Different doses of MiPLA-1 were injected (i.v.) to examine toxic effects in mice. After the injection, the mice were less active and looked ill. At doses of 7.5–10 μg/g or higher, dark urine was observed for experimental mice, but the urine from control mice remained clear. The dark color could be due to either myoglobin or hemoglobin in the urine. To determine the identity of the colored protein, we analyzed the dark urine

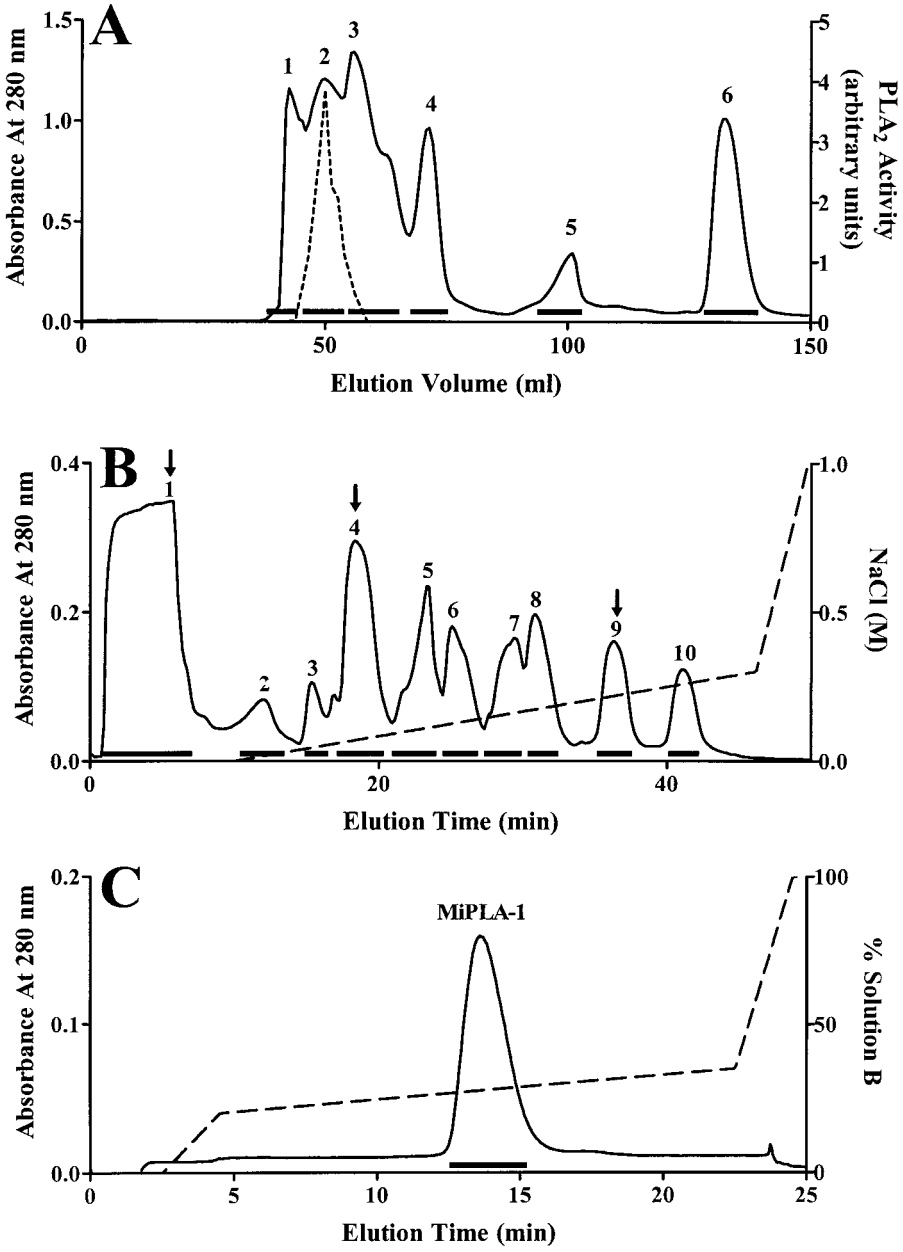

FIG. 1. Separation and purification of MiPLA-1. (A) Gel filtration of *Micropechis ikaheka* venom on a Superdex 30 column (Hiload 16/60). The column was equilibrated and eluted with 50 mM Tris–HCl buffer, pH 7.4. *M. ikaheka* venom (100 mg) was dissolved in 1 ml of 50 mM Tris–HCl buffer, pH 7.4, and centrifuged at 3000 rpm for 10 min. Supernatant was loaded onto the column. PLA_2 activity was assayed as described under Materials and Methods (- - -). (B) Ion-exchange chromatography of peak 2 from the Superdex 30 column on a FPLC UNO S1 column. Peak 2 from Superdex 30 was separated on an UNO S1 column, equilibrated, and run with 50 mM Tris–HCl buffer, pH 7.4. The elution was achieved with a linear gradient of NaCl. The PLA_2 activity was mainly associated with peaks 1, 4, and 9 (indicated by arrows). (C) Reverse-phase chromatography of peak 9 from the UNO S1 column on a Sephasil C8 column. The column was equilibrated with Solution A (0.1% TFA) and eluted with a linear gradient of Solution B (80% acetonitrile in 0.1% TFA). The bars indicated the pooled protein peaks.

using SDS–PAGE. As shown in Fig. 4, no protein band was found in the urine of control mice, while several protein bands were observed for the dark urine. The two main protein bands of dark urine had apparent molecular weights of 20 and 75 kDa, respectively. The migration pattern of the 20-kDa band was similar to that of mouse hemoglobin, but very different from those of dog and horse myoglobin. To further confirm the identity of the 20-kDa protein component, this band was transferred to a PVDF membrane and the

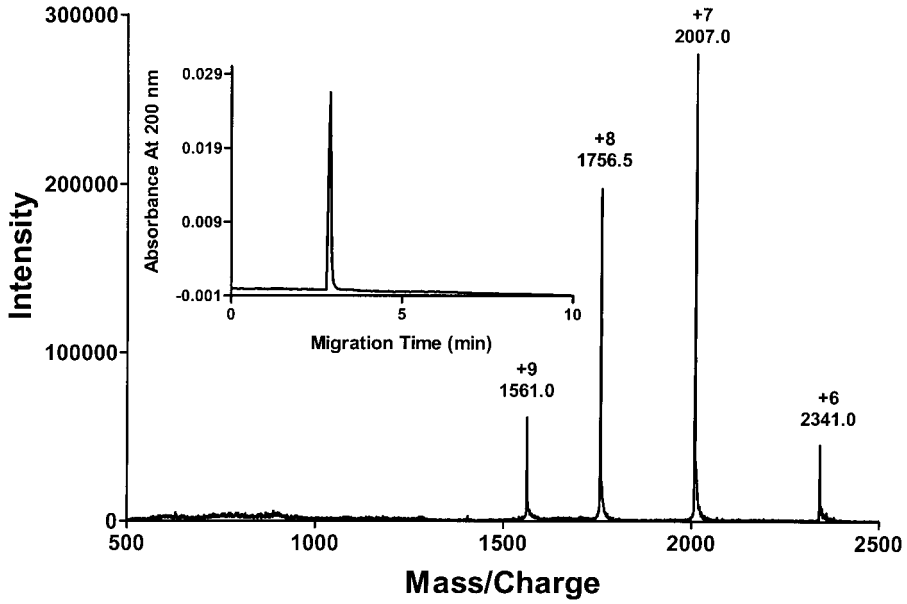

FIG. 2. Homogeneity of MiPLA-1. Electrospray mass spectrometry of MiPLA-1. The spectrum of MiPLA-1 shows a series of multiply charged ions, related to molecules bearing six to nine protons. (Inset) The purity of MiPLA-1 as determined by capillary zone electrophoresis.

N-terminal amino acid sequences were determined. It showed two parallel sequences: VLSGEDKSNI and VHFTAEEKAA. The sequences are same as the N-terminal sequences of mouse hemoglobin α and β subunits, respectively. Therefore, we conclude that the 20-kDa protein band is hemoglobin and the dark color of urine in experimental mice is due to hemoglobin. The 75-kDa protein is most likely mouse serum albumin based on its molecular weight.

Since the erythrocytes are the primary source of hemoglobin, as the first step to understand the mechanism of hemoglobinuria induced by MiPLA-1, we examined the direct hemolytic activity of MiPLA-1. As shown in Fig. 5, MiPLA-1 had no hemolytic effect on

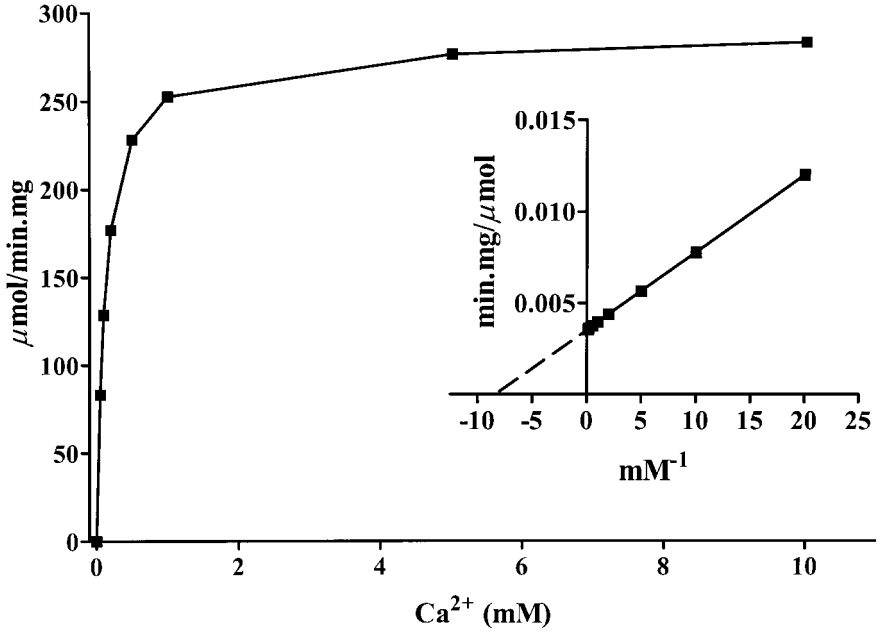

FIG. 3. Effect of Ca^{2+} on PLA_2 activity of MiPLA-1. The hydrolytic activity of MiPLA-1 on phosphatidylcholine was assayed under different Ca^{2+} concentration. (Inset) A double-reciprocal plot of the data to determine the K_d of Ca^{2+} binding to MiPLA-1.

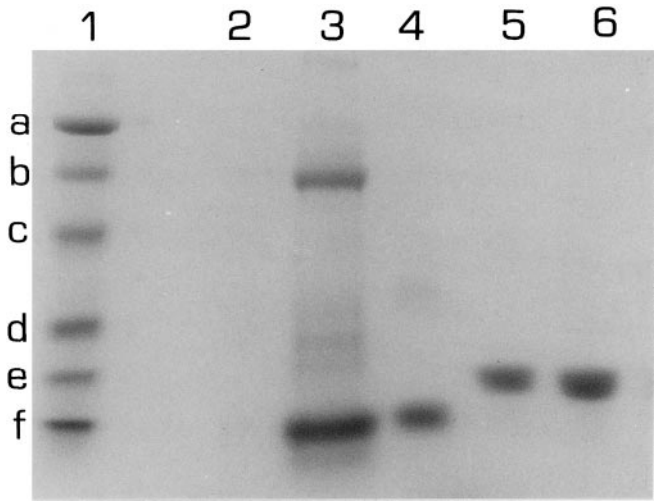

FIG. 4. SDS–polyacrylamide gel electrophoresis of mouse urine. SDS–PAGE analysis of mouse urine was performed in a Bio-Rad precast gradient gel (10–20%) under reduced conditions: lane 1, prestained molecular weight marker: (a) phosphorylase B (107 kDa), (b) bovine serum albumin (74 kDa), (c) ovalbumin (49.3 kDa), (d) carbonic anhydrase (36.4 kDa), (e) soybean trypsin inhibitor (28.5 kDa), and (f) lysozyme (20.9 kDa); lane 2, 10 μl control mouse urine; lane 3, 10 μl mouse red urine; lane 4, 10 μg mouse hemoglobin; lane 5, 10 μg dog myoglobin; lane 6, 10 μg horse myoglobin.

washed mouse erythrocytes. However, it showed a weak hemolytic activity on citrated mouse blood. Weak hemolysis can be observed at lower doses and reached about 2% hemolysis at the dose of 10 μg/ml. These results suggest that MiPLA-1 induces hemolysis through some plasma components, mostly the plasma

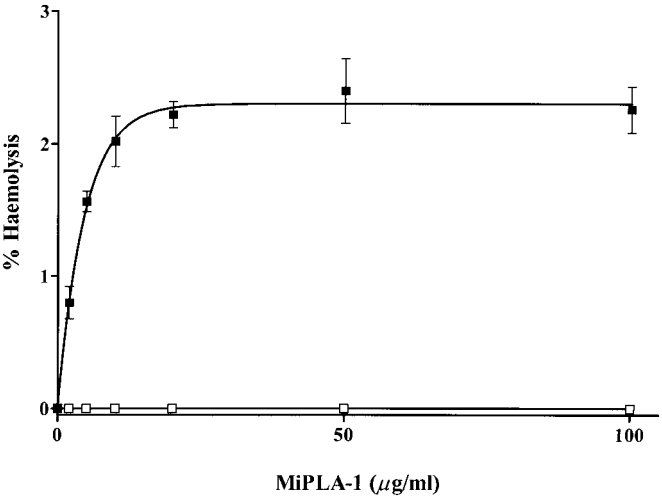

FIG. 5. Haemolytic effect of MiPLA-1. Citrated mouse blood (■) and washed mouse red erythrocyte suspension (□) were incubated with different concentrations of MiPLA-1 at 37°C for 30 min. The release of hemoglobin was measured at 540 nm and expressed as percentages of 100% hemolysis obtained by adding 1% Triton X-100. Results are presented as means ± SD (n = 3).

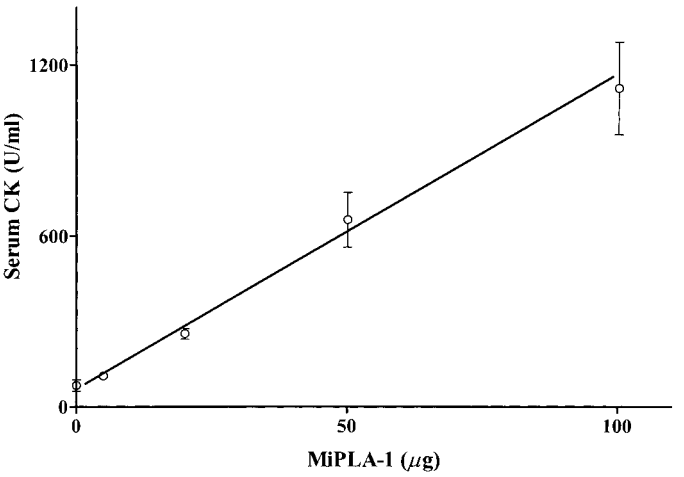

FIG. 6. Serum CK level of mice injected with MiPLA-1. Change in serum creatine kinase levels after im injection with different doses of MiPLA-1 in 100 μl 0.9% (w/v) sodium chloride. Controls were injected with 100 μl of 0.9% (w/v) sodium chloride. Results are presented as means ± SD (n = 3).

phospholipid or lipoprotein. MiPLA-1 may hydrolyze plasma phospholipid or lipoprotein and the generated lypophospholipid induces the hemolysis. However, there is no further increase in the hemolytic activity even at higher concentrations. Thus, it appears that hemoglobinuria induced by MiPLA-1 is not due to its hemolytic effects on erythrocytes.

Myotoxic Activity of MiPLA-1

Purified MiPLA-1 induced a dose-dependent myonecrosis upon i.m. injection in mice, as evidenced by the significant increase in serum CK activity (Fig. 6). At the dose of 100 μg/mouse, the serum CK level showed an increase up to 15 times in comparison to the control value. Compared with PA myotoxin from *P. australis* venom, which showed a 70 times increase in the serum CK level after local injection with the same dose (20), MiPLA-1 shows a weak myotoxic activity. Light microscopic studies also showed obvious morphological changes in skeletal muscle induced by MiPLA-1 (data not shown), including: (a) hypercontraction of myofibrils with shrunken dark areas of clumped material, (b) disruption of the myofibrils with delta lesions, and (c) vacuolation of the muscle cells which are normally found in the necrosis induced by elapid myotoxic PLA_2s (28).

Effects of MiPLA-1 on Blood Coagulation and Platelet Aggregation

Purified MiPLA-1 prolonged the clotting time of rabbit plasma. As shown in Fig. 7A, a weak effect on prothrombin time was observed under the lower dose of

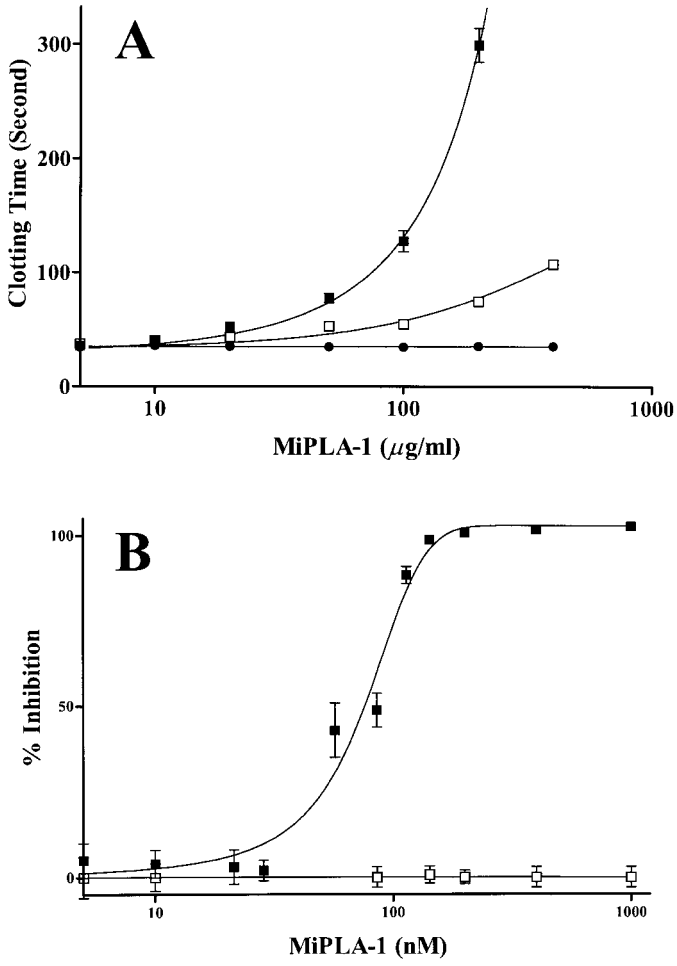

FIG. 7. Effects of MiPLA-1 on blood coagulation. (A) Effects of MiPLA-1 on prothrombin time (■), Stypven time (□), and thrombin time (●) of normal rabbit plasma. Control clotting times: 18.6 ± 0.40 s (prothrombin time), 22.2 ± 0.76 s (Stypven time), and 35.2 ± 0.32 s (thrombin time). (B) Anti-platelet effect of MiPLA-1. Platelet-rich plasma (■) and washed platelets (□) were incubated for 2 min at 37°C with MiPLA-1. Then, 4 μg/ml collagen was added and the reaction was proceed for 5 min and the extent of aggregation was expressed as the percentage of control (in the absence of MiPLA-1). All results are presented as means ± SD (n = 3).

MiPLA-1 (<10 μg/ml). With the increase of MiPLA-1, the prothrombin time was rapidly prolonged and no clotting was recorded at concentrations higher than 200 μg/ml. We also examined its effects on Stypven and thrombin time. As expected, it failed to inhibit thrombin time and a very weak effect on Stypven time was found even at high doses (>10 μg/ml). This is similar to the effects of the weak anticoagulant PLA_2 enzymes, CM-I, CM-II (29), and superbins I and II (30).

MiPLA-1 also showed a marked inhibitory effect on platelet aggregation. We studied the dose response of MiPLA-1 on platelet aggregation induced by collagen in rabbit PRP. The IC_{50} of MiPLA-1 on collagen-induced platelet aggregation was about 85.7 nM. The effect of MiPLA-1 on platelet aggregation in the washed platelet suspension was also studied. Interestingly, no antiplatelet effect of MiPLA-1 was found even up to 1 μM of MiPLA-1 (Fig. 7B). These results indicate that MiPLA-1 is similar to the antiplatelet PLA_2 purified from the venom of *Austrelaps superba*, which inhibited platelet aggregation through some plasma factors (31, 32).

Amino Acid Sequence of MiPLA-1

MiPLA-1 was reduced and pyridylethylated prior to sequence analysis. By automated Edman degradation, the first 50 residues of MiPLA-1 were identified. To determine the whole sequence of MiPLA-1, pyridylethylated MiPLA-1 was treated with cyanogen bromide and endoproteinase Lys-C and Glu-C. The generated peptides were purified with reverse-phase chromatography (Fig. 8). All peptides that were sequences are shown in Table I. The molecular weights of the sequenced peptides were determined by mass spectrometric analysis and their values matched the calculated masses deduced from the sequences of respective peptides. The complete sequence of MiPLA-1 is shown in Fig. 9A. It is a 124-amino-acid single-chain protein, without any posttranslational modification, since the calculated molecular weight value of native, PE-protein and generated peptides corresponded to the molecular weight obtained from mass spectral analysis (Table I). The amino acid sequence and the location of 14 half-cystine residues were typical of elapid and hydrophid venom PLA_2s, as well as mammalian pancreatic PLA_2s. In addition, the loop between helix C and the β-wing, which is found in pancreas PLA_2 and aptly named the "pancreatic loop," is found in the sequence of MiPLA-1. This loop is generally missing in most elapid and hydrophid venom PLA_2s. Hence, MiPLA-1 is classified as a group IB PLA_2 enzyme (33–35).

The amino acid sequence of MiPLA-1 was aligned with selected PLA_2s of group IB and its similarity was shown in Fig. 9B. Moderate similarity is found between MiPLA-1 and other group IB PLA_2s (around 55–70%). However, the pancreatic loop region (residues 59–71) shows much lower similarity (23–54%). Interestingly, two segments flanked by proline brackets are found in the sequence of MiPLA-1: PGREP (residues 14–18) and PECKGILSRP (residues 59–68). According to the predicative method described by Kini and Evans, such short segments may play an important role in protein–protein interaction (44).

DISCUSSION

Several snake venom PLA_2s have been reported to induce dark urine in snake-bite patients and experimental mice after envenomation, such as Mulgotoxin,

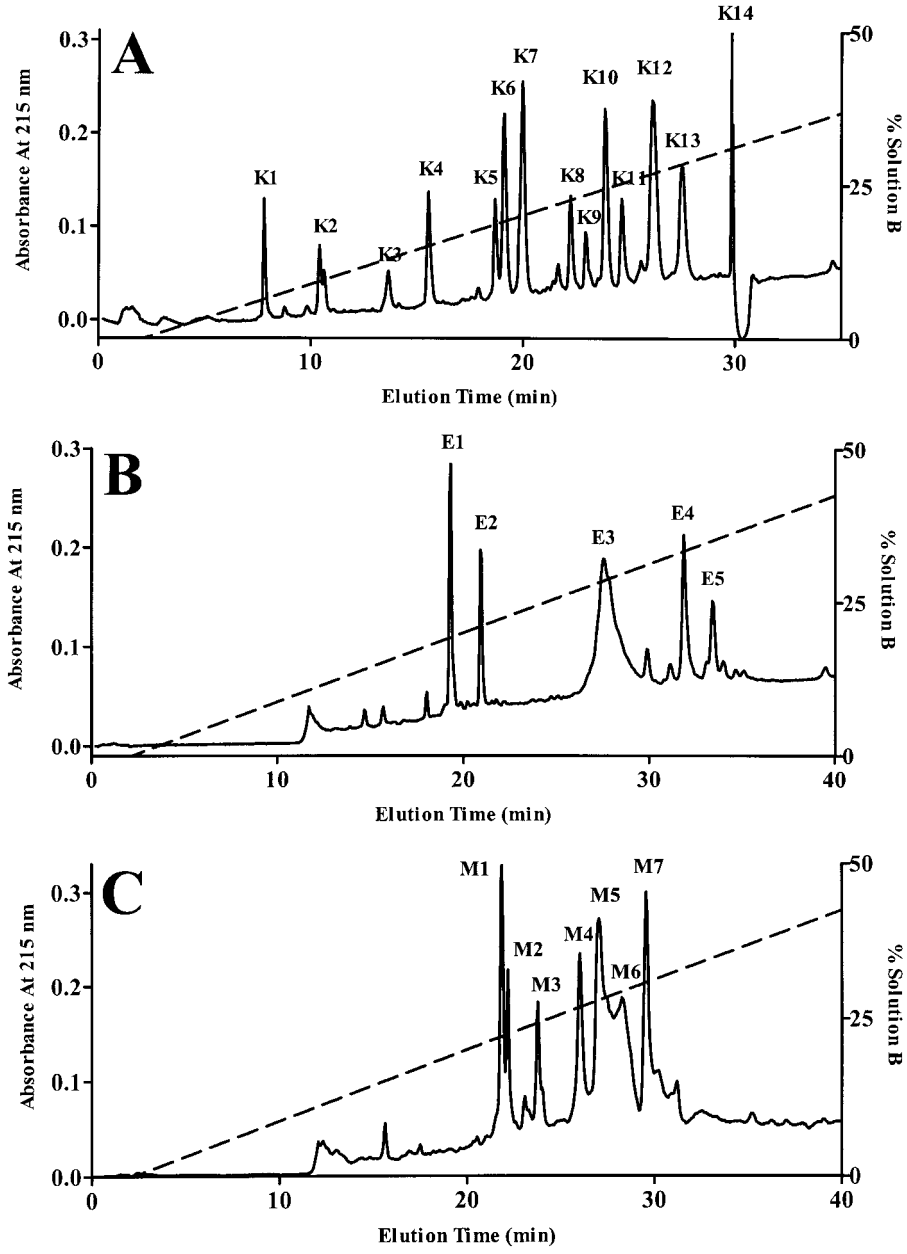

FIG. 8. RP-HPLC of digested PE-MiPLA-1. PE-MiPLA-1 was treated with endoproteinase Lys-C (A), Glu-C (B), and cyanogen bromide (C). The generated peptides were separated on C18 column of the Smart System. The column was equilibrated with Solution A (0.1% TFA) and eluted with a linear gradient of Solution B (80% acetonitrile in 0.1% TFA).

P. australis VIII-A (17, 18), and some PLA_2 homologues purified from *P. australis* venom (16). Mulgotoxin and *P. australis* VIII-A induced myoglobinuria through severe muscle damage. Previously, we also found that the nephrotoxic effects induced by *P. australis* myotoxin are due to myoglobin released by severe myotoxicity (19, 20). The myoglobin (released by a myotoxic effect) precipitates to form casts resulting in obstructive nephropathy and tubular leak. Some PLA_2 enzymes also purified from *P. australis* venom were reported to induce hemoglobinuria (16). However, the authors did not provide any experimental evidence to show that dark color of the urine was due to hemoglobinuria. Due to the lack of direct evidence, it is possible that similar to Mulgotoxin and *P. australis* VIII-A, these PLA_2 enzymes also induced myoglobinuria but not hemoglobinuria. In contrast to *P. australis* PLA_2 enzymes, MiPLA-1 induces hemoglobinuria but not

TABLE I

Mass Analysis of Native, PE-MiPLA-1, and Sequenced Peptides

Peptide	Residues	Calculated[a]	Observed[b]
Native MiPLA-1	1–124	14,041.04	14,041.60 ± 1.78
PE-MiPLA-1	1–124	15,527.00	15,525.80 ± 0.49
	Lys-C-digested peptides		
K1	82–88	926.05	925.80 ± 0.55
K2	58–62	693.85	693.45 ± 0.17
K4	109–121	1,540.68	1,540.49 ± 0.53
K6	32–54	2,829.06	2,828.78 ± 0.05
K7	1–7	918.10	918.00 ± 0.55
K8	93–108	2,122.61	2,122.41 ± 1.10
K9	63–79	2,069.33	2,071.11 ± 0.68
K12	11–31	2,595.00	2,595.09 ± 0.37
	Glu-C-digested peptides		
E1	41–60	2,697.03	2,696.68 ± 0.32
E3	61–113	6,816.04	6,816.53 ± 2.16
E4	1–40	4,667.38	4,667.31 ± 0.38
	CNBr-digested peptides		
M1	104–124	2,588.02	2,588.19 ± 0.86

Note. All cysteine residues were pyridylethylated except native protein.

[a] Molecular masses were calculated from the amino acid sequences of these fragments.

[b] Molecular masses were determined by electrospray mass spectrometry.

myoglobinuria. Thus, MiPLA-1 is the first hemoglobinuria-inducing toxin known from snake venom and it may contribute to the dark urine observed in the patient bitten by this kind of snake (1).

To elucidate the mechanism of hemoglobinuria, we examined the hemolytic activity of MiPLA-1. The results indicated that MiPLA-1 had no effect on washed mouse erythrocytes but had a weak effect on whole blood. The percentage of hemolysis can only reach 2% even at high concentrations (100 μg/ml). This weak hemolytic effect may depend on the hydrolysis of plasma phospholipid or lipoprotein by MiPLA-1 and the released lypophospholipid induces the hemolysis of mouse erythrocytes. Most of the PLA_2 enzymes exhibit this hydrolytic activity and induce indirect hemolysis. But this weak hemolysis cannot explain why MiPLA-1 induces hemoglobinuria. Currently, it is not clear whether this phenomenon is due to a direct action of MiPLA-1 on kidney function. The presence of several proteins, including hemoglobin and serum albumin, in the dark-colored urine supports this contention. According to a hypothetical model the venom PLA_2s target the specific tissue or cell due to their affinity toward specific proteins rather than lipid domains (45). After the initial binding, PLA_2s induce various pharmacological effects by mechanisms that are either dependent on or independent of their enzymatic activity. Identification of high-affinity receptors for PLA_2s in different tissues and cultured cells (for example, Refs. 46 and 47) strongly supports this model. We speculate that the kidney may be one target organ of MiPLA-1; after i.v. injection, it may bind to kidney cells and induce the kidney leakage which results in hemoglobinuria. Further studies are underway to elucidate its effect on kidney function.

Beside hemoglobinuria, purified MiPLA-1 also showed a wide range of biological effects, including myotoxicity as well as antiplatelet and anticoagulant effects. MiPLA-1 strongly inhibited the platelet aggregation in PRP induced by collagen, with an IC_{50} value of about 85.7 nM, but its inhibitory effect totally disappeared when we examined its effect on washed platelet suspension. This is similar to the snake venom PLA_2 enzyme described by Yuan *et al.* (31, 32); its inhibitory effect was dependent on hydrolysis of plasma lipoprotein. Blood coagulation assays have shown that it has anticoagulant effect on the prothrombin time, but has no significant effect on Stypven and thrombin times of normal plasma. Hence, MiPLA-1 may inhibit the extrinsic tenase complex but not the prothrombinase (29). Thus, MiPLA-1 may also contribute to the anticoagulant effect of *M. ikaheka* snake-bite patients.

As the first step of understanding the structure–function relationship of MiPLA-1, its complete sequence was determined. The results indicated that MiPLA-1 is a 124-amino-acid protein. Based on the complete amino acid sequence, the residues involved in the catalytic network (H48, D99, Y52, and Y73) (48, 49) and Ca^{2+} binding (Y28, G30, G32, and D49) (49–51) are highly conserved in MiPLA-1. It is noteworthy that MiPLA-1 possesses the pancreatic loop at residues 62–66, which is found in pancreas PLA_2s but is missing from most snake venom PLA_2s. Among sequenced snake venom PLA_2s, only a few enzymes from elapids contain residues in this pancreatic loop. They are the γ-subunit of taipoxin (42), the D subunit of textilotoxin (43), OS1 (40), HTe (39), and OHV A-PLA_2 (41). Like OS1, HTe, and OHV A-PLA_2, neither a propeptide-like peptide nor additional half-cystines are found in the sequence of MiPLA-1 as they are found in γ-subunit of taipoxin and D subunit of textilotoxin.

Over the past 20 years, X-ray crystallography and protein engineering have been widely used to study the structure–function relationship of PLA_2. Three-dimensional structures of several pancreatic and snake venom PLA_2s have been reported (51–55). All these enzymes show a remarkable similarity in their three-dimensional structures. The results also indicate that

(A)

```
NLLQFRKMIKCTVPGREPLVAFTDYGCYCGKGGSGTPVDELDRCCQTHDNCYDKAEKLPECKGILSRPYVNTYAYDCTKGKITCN
                                          \-------E1---------/\-----------------------
\------------------N-terminal-----------------/        \K2/

DQKDKCKLFICNCDRTAAMCFAKARYIEANNHIDPKRCK
------E3-------------------/
                  \---------M1-------/
```

(B)

	10	20	30	40	50	60
1. MiPLA-1	NLLQFRKMIK	CTVPGREPLV	AFTDYGCYCG	KGGSGTPVDE	LDRCCQTHDN	CYDKAEKLPE
2. b. pancreas	ALWQFNGMIK	CKIPSSEPLL	DFNNYGCYCG	LGGSGTPVDD	LDRCCQTHDN	CYKQAKKLDS
3. p. pancreas	ALWQFRSMIK	CAIPGSHPLM	DFNNYGCYCG	LGGSGTPVDE	LDRCCETHDN	CYRDAKNLDS
4. HTe	NLYQFGNMIQ	CANHGRRPTR	HYMDYGCYCG	KGGSGTPVDE	LDRCCQTHDD	CYGEAEKLPA
5. OS1	SLLNFANLIE	CANHGTRSAL	AYADYGCYCG	KGGRGTPLDD	LDRCCHVHDD	CYGEAEKLPA
6. OHV A-PLA_2	HLIQFGNMIQ	CTVPGFLSWI	KYADYGCYCG	AGGSGTPVDK	LDRCCQVHDN	CYTQAQKLPA
7. Textilo. D	NIMLFGNMIQ	CTIPCEQSWL	GYLDYGCYCG	SGSSGIPVDD	VDKCCKTHDE	CYYKAGQIPG
8. Taipoxin γ	DFEQFSNMIQ	CTIPCGSECL	AYMDYGCYCG	PGGSGTPIDD	LDRCCKTHDE	CYAEAGKLSA

	70	80	90	100	110	120	Similarity (%)
1.	CKGILSRPYV	NTYAYDCTKG	KITCNDQKDK	CKLFICNCDR	TAAMCFAKAR	YIEANNHIDP ---KRCK	
2.	CKVLVDNPYT	NNYSYSCSNN	EITCSSENNA	CEAFICNCDR	NAAICFSKVP	YNKEHKNLDK ----NC	60.5
3.	CKFLVDNPYT	ESYSYSCSNT	EITCNSKNNA	CEAFICNCDR	NAAICFSKAP	YNKEHKNLDT K--KYC	58.9
4.	CNYMMSGPYY	NTYSYECNEG	ELTCKDNNDE	CKAFICNCDR	TAAICFARAP	YNDANWNIDT K--TRCQ	69.4
5.	CNYLMSSPYF	NSYSYKCNEG	KVTCTDDNDE	CKAFICNCDR	TAAICFAGAT	YNDENFMISK KYNDICQ	63.4
6.	CSSIMDSPYV	KIYSYDCSER	TVTCKADNDE	CAAFICNCDR	VAAHCFAASP	YNNNNYNIDT T--TRC	61.3
7.	CSVQPNEVFN	VDYSYECNEG	QLTCNESNNE	CEMAVCNCDR	AAAICFARFP	YNKNYWSINT E--IHCR	55.6
8.	CKSVLSEPNN	DTYSYECNEG	QLTCNDDNDE	CKAFICNCDR	TAVTCFAGAP	YNDDLYNIGM I---ECHK	63.7

FIG. 9. Amino acid sequence determination of MiPLA-1 and sequence comparison. (A) The sequence of MiPLA-1 is shown along with the cleavage sites for endoproteinases digestion and cyanogen bromide treatment employed to produce peptides. Only selected overlapping peptides needed to support the structure are shown. (B) Comparison of the amino acid sequence of MiPLA-1 aligned with selected PLA2s. The common number system defined by Renetseder *et al.* is used (36). The PLA_2s are from bovine pancreas (37), porcine pancreas (38), *Notechis scutatus scutatus* (HTe) (39), *Oxyranus scutellatus scutellatus* (OS_1 and taipoxin γ subunit) (40, 42), OHV A-PLA_2 (41), and *Pseudonaja textilis* (Textilo. D) (43). N-terminal residues 1–8 of textilotoxin D and taipoxin γ are not shown.

sequence around the pancreatic loop plays an important role in the conformation and hydrolytic activity of PLA_2 (56–59). Comparison of the crystal structure of bovine and porcine pancreatic PLA_2s shows a remarkable conformational difference in the pancreatic loop region from residue 59 to residue 71 (51, 52), although these two enzymes have 85% identity in their amino acid sequences. The cause of this large conformation difference has been attributed to a single substitution at position 63 (56). The experiment data proved that the single Phe → Val substitution at position 63 of porcine pancreatic PLA_2 caused a large conformational change and resulted in a conformation more close to that of bovine PLA_2 than that of porcine PLA_2 (57). Removal of the surface loop (residues 62–66) of porcine pancreatic PLA_2 resulted in a conformation more like that of snake venom PLA_2 and enhanced activity more than wild-type PLA_2 (58, 59). MiPLA-1 has a moderate similarity with other group IB PLA_2s (around 55–70%), but the sequence around the pancreatic loop region (59–71) are very different with the similarities: bovine pancreas PLA2 (53.8%), porcine (46.2%), HTe (46.2%), OS1 (53.8%), OHV A-PLA_2 (46.2%), textilotoxin D (23.1%), and taipoxin γ (46.2%). Based on this low similarity, we expect significant structural differences in this region.

Recently, based on the observation that proline is the most common residue in the flanking segments of interaction sites (60), Kini and Evans developed a unique predictive method to determine protein–protein interaction (44). These proline residues act as distinct barriers between the interaction sites and their neighbouring segments. Hence, they protect the integrity and conformation of the active site (60). This method

has been successfully applied to identify several protein–protein interaction sites (44, 61, 62). It is important to note that two short segments flanked by proline brackets are found in the sequence of MiPLA-1:PGREP (residues 14–18) and PECKGILSRP (residues 59–68). Both of these segments are on the surface of the molecule (data not shown). It will be interesting to test whether these segments play important roles in one of the biological activities.

ACKNOWLEDGMENTS

The authors thank Dr. Geraldine Chow and Jeremiah S. Joseph from Bioscience Centre, National University of Singapore, for their kind assistance in determination of masses and sequences of proteins and peptides. Rong Gao is a recipient of a research scholarship from the National University of Singapore.

REFERENCES

1. Warrell, D. A., Hudson, B. J., Lalloo, D. G., Trevett, A. J., Whitehead, P., Bamler, P. R., Ranaivoson, M., Wiyono, A., Richie, T. L., Fryauff, D. J., O'Shea, M. T., Richards, A. M., and Theakston, R. D. G. (1996) *Q. J. Med.* **89,** 523–530.
2. Blasco, P., and Hornabrook, R. W. (1972) *Papua New Guinea Med. J.* **15,** 155–156.
3. Lai, C. M. D., Chow, G., and Kini, R. M. (1997) *in* Proceedings of Science Research Congress, Singapore, pp. 417–422.
4. Geh, S. L., Vincent, A., Rang, S., Abrahams, T., Jacobson, L., Lang, B., and Warrell, D. A. (1997) *Toxicon* **35,** 101–109.
5. Kamiguti, A. S., Treweeke, A. T., Lowe, G. M., Laing, G. D., Theakston, R. D. G., Warrell, D. A., and Zuzel, M. (1995) *Toxicon* **33,** 275.
6. Strong, P. N., Goerke, J., Oberg, S. G., and Kelly, R. B. (1976) *Proc. Natl. Acad. Sci. USA* **73,** 178–182.
7. Gopalakrishnakone, P., Dempster, D. W., Hawgood, B. J., and Elder, H. Y. (1984) *Toxicon* **22,** 85–98.
8. Lee, C. Y., Hod, C. L., and Eaker, D. (1977) *Toxicon* **15,** 355–356.
9. Verheij, H. M., Boffa, M. C., Rothen, C., Bryckaert, M. C., Verger, R., and de Haas, G. H. (1980) *Eur. J. Biochem.* **112,** 25–32.
10. Chen, R. H., and Chen, Y. C. (1989) *Toxicon* **27,** 675–682.
11. Fletcher, J. E., Rapuano, B. E., Condrea, E., Yang, C. C., Ryan, M., and Rosenberg, P. (1980) *Biochem. Pharmacol.* **29,** 1565–1574.
12. Huang, H. C. (1984) *Toxicon* **22,** 359–372.
13. Condrea, E., Fletcher, J. E., Rapuano, B. E., Yang, C. C., and Rosenberg, P. (1981) *Toxicon* **19,** 61–71.
14. Vishwanath, B. S., Kini, R. M., and Gowda, T. V. (1985) *Toxicon* **23,** 617.
15. Vishwanath, B. S., Kini, R. M., and Gowda, T. V. (1987) *Toxicon* **25,** 501–515.
16. Takasaki, C., Suzuki, J., and Tamiya, N. (1990) *Toxicon* **28,** 319–327.
17. Leonardi, T. M., Howden, M. E. H., and Spence, I. (1979) *Toxicon* **17,** 549–555.
18. Mebs, D., and Samejima, Y. (1980) *Toxicon* **18,** 443–454.
19. Ponraj, D., and Gopalakrishnakone, P. (1996) *Lab. Animal. Sci.* **46,** 393–398.
20. Ponraj, D., and Gopalakrishnakone, P. (1997) *Kidney Int.* **51,** 1956–1969.
21. Kawauchi, S., Iwanaga, S., Samejima, Y., and Suzuki, T. (1970) *Biochim. Biophys. Acta* **236,** 142–160.
22. Williams, W. J., and Esnouf, M. P. (1962) *Biochem. J.* **84,** 52–62.
23. Marrakchi, N., Barbouche, R., Guermazi, S., Bon, C., and el Ayeb, M. (1997) *Toxicon* **35,** 261–272.
24. Born, G. V. R. (1962) *Nature* **194,** 927–929.
25. Diaz, C., Alape, A., Lomonte, B., Olamendi, T., and Gutierrez, J. M. (1994) *Arch. Biochem. Biophys.* **312,** 336–339.
26. Mayer, R. J., and Marshall, L. A. (1993) *FASEB J.* **7,** 339–348.
27. Dennis, E. A. (1994) *J. Biol. Chem.* **269,** 13057–13060.
28. Ownby, C. L., and Colberg, T. R. (1988) *Toxicon* **26,** 459–474.
29. Stefansson, S., Kini, R. M., and Evans, H. J. (1989) *Thromb. Res.* **55,** 481–491.
30. Subburaju, S., and Kini, R. M. (1997) *Toxicon* **35,** 1239–1250.
31. Yuan, Y., Jackson, S. P., Mitchell, C. A., and Salem, H. H. (1993) *Thromb. Res.* **70,** 471–481.
32. Yuan, Y., Jackson, S. P., Newnham, H. H., Mitchell, C. A., and Salem, H. H. (1995) *Blood* **86,** 4166–4174.
33. Heinrikson, R. L., Krueger, E. T., and Keim, P. S. (1977) *J. Biol. Chem.* **252,** 4913–4921.
34. Dufton, M. J., and Hider, R. C. (1983) *Eur. J. Biochem.* **137,** 545–551.
35. Davidson, F. F., and Dennis, E. A. (1990) *J. Mol. Evol.* **31,** 228–238.
36. Renetseder, R., Brunie, S., Dijkstra, B. W., Drenth, J., and Sigler, P. B. (1985) *J. Biol. Chem.* **260,** 11627–11634.
37. Fleer, E. A. M., Verheij, H. M., and de Haas, G. H. (1978) *Eur. J. Biochem.* **82,** 261–269.
38. Puijk, W. C., Verheij, H. M., and de Haas, G. H. (1977) *Biochim. Biophys. Acta* **492,** 254–259.
39. Francis, B., Coffield, J. A., Simpson, L. L., and Kaiser, I. I. (1995) *Arch. Biochem. Biophys.* **318,** 481–488.
40. Lambeau, G., Ancian, P., Nicolas, J. P., Beiboer, S. H. W., Moinier, D., Verheij, H., and Lazdunski, M. (1995) *J. Biol. Chem.* **270,** 5534–5540.
41. Huang, M. Z, Gopalakrishnakone, P., Chung, M. C. M., and Kini, R. M. (1997) *Arch. Biochem. Biophys.* **338,** 150–156.
42. Fohlman, J., Lind, P., and Eaker, D. (1977) *FEBS Lett.* **84,** 367–371.
43. Pearson, J. A., Tyler, M. I., Retson, K. V., and Howden, M. E. H. (1991) *Biochim. Biophys. Acta* **1077,** 147–150.
44. Kini, R. M., and Evans, H. J. (1995) *FEBS Lett.* **375,** 15–17.
45. Kini, R. M., and Evans, H. J. (1989) *Toxicon* **27,** 613–635.
46. Lambeau, G., Lazdunski, M., and Barhanin, J. (1991) *Neurochem. Res.* **16,** 651–658.
47. Hanasaki, K., and Arita, H. (1992) *J. Biol. Chem.* **267,** 6414–6420.
48. Verheij, H. M., Volwerk, J. J., Jansen, E. H., Puyk, W. C., Dijkstra, B. W., Drenth, J., and de Haas, G. H. (1980) *Biochemistry* **19,** 743–750.
49. Scott, D. L., White, S. P., Otwinowski, Z., Yuan, W., Gelb, M. H., and Sigler, P. B. (1990) *Science* **250,** 1541–1546.
50. Van den Bergh, C. J., Slotboom, A. J., Verheij, H. M., and de Haas, G. H. (1989) *J. Cell Biochem.* **39,** 379–390.
51. Dijkstra, B. W., Kalk, K. H., Hol, W. G. J., and Drench, J. (1981) *J. Mol. Biol.* **147,** 97–123.
52. Dijkstra, B. W., Renetseder, R., Kalk, K. H., Hol, W. G. J., and Drench, J. (1983) *J. Mol. Biol.* **168,** 163–179.
53. Brunie, S., Bolin, J., Gewirth, D., and Sigler, P. B. (1985) *J. Biol. Chem.* **260,** 9742–9749.

54. Westerlund, B., Nordlund, P., Uhlin, U., Eaker, D., and Eklund, H. (1992) *FEBS Lett.* **301,** 159–164.
55. Tang, L., Zhou, Y., and Lin, Z. (1998) *J. Mol. Biol.* **282,** 1–11.
56. Dijkstra, B. W., Weijer, W. J., and Wierenga, R. K. (1983) *FEBS lett.* **164,** 25–27.
57. Thunnissen, M. M. G. M., Franken, P. A., de Haas, G. H., Drenth, J., Kalk, K. H., Verheji, H. M., and Dijkstra, B. W. (1993) *J. Mol. Biol.* **232,** 839–855.
58. Kuipers, O. P., Thunnissen, M. M. G. M., de Geus, P., Dijkstra, B. W., Drench, J., Verheij, H. M., and de Haas, G., H. (1989) *Science* **244,** 82–85.
59. Thunnissen, M. M. G. M., Kalk, K. H., Drench, J., and Dijkstra, B. W. (1990) *J. Mol. Biol.* **216,** 425–439.
60. Kini, R. M., and Evans, H. J. (1995) *Biochem. Biophys. Res. Commun.* **212,** 1115–1124.
61. Kini, R. M., and Evans, H. J. (1996) *FEBS Lett.* **385,** 81–86.
62. Kini, R. M., Caldwell, R. A., Wu, Q. Y., Baumgarten, C. M., Feher, J. J., and Evans, H. J. (1998) *Biochemistry* **37,** 9058–9063.